Journal of Cleaner Production 462 (2024) 142719

Contents lists available at ScienceDirect

Journal of Cleaner Production

journal homepage: www.elsevier.com/locate/jclepro

An innovative 'sea-thermal' synergetic biorefinery for biofuel production: Co-valorization of lignocellulosic and algal biomasses using seawater under hydrothermal conditions

Yingdong Zhou [a,b,c], Javier Remón [b,d,*], Wei Ding [e], Zhicheng Jiang [f], José Luis Pinilla [b], Changwei Hu [c,**], Isabel Suelves [b]

[a] College of Materials and Chemistry & Chemical Engineering, Chengdu University of Technology, Chengdu, 610059, PR China
[b] Instituto de Carboquímica, CSIC, Zaragoza, 50018, Spain
[c] Key Laboratory of Green Chemistry and Technology, Ministry of Education, College of Chemistry, Sichuan University, Chengdu, Sichuan, 610064, PR China
[d] Thermochemical Processes Group, Aragón Institute for Engineering Research (I3A), University of Zaragoza, C/Mariano Esquillor s/n, 50.018, Zaragoza, Spain
[e] College of New Materials and Chemical Engineering, Beijing Institute of Petrochemical Technology, Beijing, 102617, PR China
[f] College of Biomass Science and Engineering, Sichuan University, Chengdu, 610065, PR China

ARTICLE INFO

Handling Editor: Cecilia Maria Villas Bôas de Almeida

Keywords:
Microalgae
Almond hulls
Hydrothermal treatment
Seawater
Biorefinery
Co-valorization

ABSTRACT

This study explores the co-hydrothermal treatment (co-HTT) of almond hulls and *Chlorella Vulgaris* using seawater as an alternative HTT medium. The influence of the feedstock (individual biomass and all the possible binary mixtures) was systematically evaluated under different conditions (reaction temperatures and times). The feedstock mixture and hydrothermal conditions significantly influenced the overall product distribution: gas (1–5%), hydrochar (6–56%), biocrude (6–55%), and aqueous fraction (33–52%), along with the most representative physicochemical and fuel properties of these products. Notably, the biocrude had a calorific value of 24–31 MJ/kg, whereas the hydrochar shifted between 3 and 26 MJ/kg. The degradation of abundant polysaccharides in almond hulls produced acidic species, promoting the degradation of proteins to N-containing species in biocrude. The synergies between microalgae and almond hulls favored the deamination of amino acid and repolymerization of formed monomers. Process optimization revealed that the best biocrude production (59% yield and HHV = 28 MJ/kg) was obtained by treating *C. Vulgaris* at 268 °C for 180 min. Contrarily, the HTT of almond hulls under optimum processing conditions (300 °C and 112 min) also produced an energy-dense biocrude (29 MJ/kg) but with a much lesser yield (16%). However, such a low biocrude production can be synergistically increased up to 33 %, maintaining the HHV (31 MJ/kg), including up to 61 wt% of *C. Vulgaris* into the feedstock, with a feedstock energy recovery of 75%. Holistically, the co-HTT of 40 wt% *C. Vulgaris* and 60 wt % almond hulls at 300 °C for 180 min produced energy-dense liquid (23% yield and HHV = 32 MJ/kg) and solid (29% yield and HHV = 25 MJ/kg) biofuels simultaneously, with a feedstock energy recovery of 80%. Given these excellent prospects, this strategy provides timely and new insights into developing synergetic strategies to utilize microalgal and lignocellulosic biomasses more efficiently, paving the way toward developing holistic and unseasonal biorefinery processes.

1. Introduction

Growing mechanization and development have dramatically increased energy and chemical consumption over the past few years (Zhou et al., 2022a). Currently, approximately 80% of the world's energy is produced from limited fossil resources, which are responsible for several environmental issues (e.g., global warming and exhaust gas emissions) (Sahoo et al., 2021; Xu et al., 2018). Given this energetic picture, developing green and sustainable biofuels and energy carriers have become a pressing challenge to palliate environmental concerns. In the short term, obtaining biofuels and biochemicals from biomass feedstocks, wastes, and industrial by-products is considered an

* Corresponding author. Instituto de Carboquímica, CSIC, Zaragoza, 50018, Spain.
** Corresponding author.
E-mail addresses: jrn@unizar.es (J. Remón), changweihu@scu.edu.cn (C. Hu).

https://doi.org/10.1016/j.jclepro.2024.142719
Received 19 February 2024; Received in revised form 21 May 2024; Accepted 27 May 2024
Available online 28 May 2024
0959-6526/© 2024 The Authors. Published by Elsevier Ltd. This is an open access article under the CC BY-NC license (http://creativecommons.org/licenses/by-nc/4.0/).

attractive and up-and-coming option due to their carbon-neutral nature and intrinsic ability to generate fewer greenhouse gases than fossil fuels (Nigam and Singh, 2011; Yang et al., 2019). Among the different biomass resources, lignocellulosic wastes and algae are promising candidates for obtaining fuels and chemicals (Obeid et al., 2019; Zhou et al., 2020). Besides, they are readily available, have a short growth cycle, and can reduce carbon dioxide emissions. Chemically, lignocellulosic biomasses mainly comprise cellulose, hemicellulose and lignin, whereas algae are abundant in lipids, saccharides, and proteins (Gai et al., 2015; Li et al., 2022).

As regards the effective and sustainable transformation of these feedstocks into valuable products, thermochemical conversion technologies (pyrolysis, gasification, and hydrothermal treatment) are attractive to produce a varied spectrum of valuable chemicals and energy-dense biofuels and precursors from microalgal and lignocellulosic biomasses (Ong et al., 2019, 2020). Among these processes, hydrothermal treatment (HTT) has gained plenty of attention because it produces biocrude (an energy-dense biofuel), hydrochar (a sustainable biomaterial and biofuel), and gaseous and aqueous products (biochemicals) simultaneously (Zhou et al., 2023). Additionally, it avoids the feedstock drying required by other conversion techniques, which increases the energetic profitability of this methodology (Remón et al., 2021a, 2021b). HTT is generally conducted in an aqueous medium under sub- or supercritical conditions (150–400 °C, 5–25 MPa), with generally higher biocrude yields than other thermochemical routes (Galadima and Muraza, 2018; Hu et al., 2019; Zhou and Hu, 2020). Despite these promising features, the bottleneck for developing and implementing this technology relies on its high feedstock dependence, i.e., the conversion and product yields and properties highly depend on the type of biomass. Concerning lignocellulosic and algal biomasses, recent studies indicate that the biocrudes yielded from the HTT of lignocellulosic biomass are usually much lower than those from algal biomass because the components in algae (lipid, carbohydrates and proteins) are more active than lignocelluloses (Gai et al., 2015; Remón et al., 2020; Yang et al., 2019). Besides, algae contain a high fraction of proteins, resulting in a biofuel containing a high amount of nitrogen, which could harm the environment due to possible NO_x formation (Galadima and Muraza, 2018; Guo et al., 2015; Zhou et al., 2020; Zhou and Hu, 2020).

Driven by the pros and cons linked to the HTT of single feedstocks, the co-hydrothermal treatment (co-HTT) of different biomasses (e.g., lignocellulosic and algal biomass) arises as a viable option to enhance the conversion efficiency and control the distribution of the products (Leng et al., 2020; Sahoo et al., 2021; Yang et al., 2019). Additionally, this co-valorization philosophy contributes toward developing season-free and more flexible biorefinery processes. Therefore, the co-HTT of different feedstocks, such as lignocellulosic with algal biomass, micro-with macroalgae, and mixed culture of microalgal species, is an emerging and trendy strategy with a promising future (Dandamudi et al., 2017; Gai et al., 2015; Jin et al., 2013). In this respect, Hu and coworkers reported on the co-HTT of algae and sawdust in ethanol-water co-solvent (Hu et al., 2018). The results showed positive synergetic influences during the co-processing of both resources. In another work, Gai et al. studied the impact of some reaction parameters (temperature, residence time, solid concentration and mass ratio of algae/lignocelluloses) on the co-HTT of microalgae and rice husk in subcritical water. These authors found synergistic interactions between these feedstocks, where the generated intermediates/products from one feedstock could intervene in the conversion pathway of the other, leading to an enhanced biocrude yield, improved biocrude acidity, and N content. In this regard, the cost of the downstream processing (upgradation) of the products could be alleviated, leading to an enhanced economic benefit in Co-HTT (Fakudze and Chen, 2023; Gai et al., 2015; Sahoo et al., 2021).

In addition to these trendy co-valorization strategies, developing appropriate catalysts is also paramount. During the HTT of biomass, water simultaneously behaves as a solvent, reactant, and catalyst under subcritical conditions. Therefore, a substantial number of works addressing the HTT of lignocellulosic and algal biomasses have been conducted without a catalyst (Dimitriadis and Bezergianni, 2017; Elliott et al., 2015; Seshasayee and Savage, 2021). However, using homogeneous or heterogeneous catalysts can be more advantageous in improving product yields and enhancing their physicochemical and fuel properties. Homogeneous catalysts have included alkali salts (Na_2CO_3, K_2CO_3, and $KHCO_3$) (Hongthong et al., 2020; Sharma et al., 2021), while heterogeneous catalysts comprised metals (Ni, Pt, Pd and Ru) supported on different materials (NiO, ZnO, MnO, MgO, CeO_2, La_2O_3, zeolites and carbon materials) (Elliott et al., 2015; Hongthong et al., 2020; Toor et al., 2011; Zhou et al., 2021). In general terms, homogeneous catalysts are typically more active but more difficult to recycle. Conversely, heterogeneous catalysts allow for a more straightforward recovery but are less effective due to limitations in mass transfer (biomass-catalyst) (Hongthong et al., 2020).

Accounted for by these catalytic singularities, autocatalytic and more sustainable reaction media can also be a green and abundant alternative for expanding and accelerating novel hydrothermal co-valorization strategies. In this respect, one significant concern of HTTs is that they consume much freshwater (2–6 m^3 freshwater/m^3 biofuel) (Fang et al., 2015). Thus, considering the overpopulation picture worldwide, the freshwater shortage in some countries and/or areas limits the conversion of biomass via a HTT strategy using fresh water. As the most abundant undrinkable water on the planet, seawater arises as a potential reaction medium for the HTT of biomass. It is abundant in inorganic salts, e.g., chlorides (NaCl, KCl, $CaCl_2$, and $MgCl_2$), carbonates ($NaHCO_3$), and sulfates ($MgSO_4$) and which exert promotion and catalytic impacts in biomass conversion (Domínguez de María, 2013). Given these opportunities, seawater as an alternative HTT medium in biomass conversion is viable and sustainable in replacing (totally or partially) freshwater and chemical catalysts.

Despite these favorable prospects, only a handful of recent publications have addressed the seawater-assisted HTT of lignocellulosic biomass, while the HTT of algal biomass or mixtures of them is unreported. Additionally, most of these studies were directed toward biomass conversion to valuable chemicals (Grande et al., 2012; Jiang et al., 2018b; Shao et al., 2020), with little work on simultaneously producing biofuels and valuable chemicals. In this latter case, Yang et al. reported on the effect of seawater on the hydrothermal liquefaction (HTL) of sawdust. Experiments conducted with binary mixtures of model compounds (cellulose, hemicellulose, and lignin) using seawater and freshwater with/without NaCl and Na_2CO_3, combined with theoretical calculations, suggested that salts in seawater had diverse impacts on the process ruling the formation and properties of the biocrude and hydrochar (Yang et al., 2022). Previous research articles explored the partial and total replacement of freshwater with seawater during the HTT of microalgae. We found that seawater showed different influences based on the reaction medium salinity. Diluted seawater favored the dissolution and depolymerization of polysaccharides and proteins in the alga by disrupting the H-bonding networks within these macromolecules due to the autocatalytic effect. In contrast, enriched seawater media promoted the deoxygenation and repolymerization of the biocrude into hydrochar (Zhou et al., 2022b, 2022c) As for almond hulls, the experimental results revealed that salts in seawater promoted biocrude formation, favoring the scission of O–H bonds in almond hulls (Remón et al., 2022a). Based on these articles, it could be concluded that seawater exerts catalytic/promotional effects during biomass HTT, which proves that using seawater as the solvent during the HTT of biomass is feasible. This work addressed the synergistic co-valorization of lignocellulosic and algal biomasses under different reaction conditions. Thus, we focused on the feedstock synergies using seawater as the reaction medium, as the promotional effect of seawater was already addressed for both feedstocks in previous publications. However, these effects vary from biomass to biomass. Thus, analyzing and revealing the

synergies between different biomasses during co-HTT using seawater as a reaction media is essential.

Given these challenges and opportunities, this work explores the synergetic co-processing of almond hulls and *Chlorella Vulgaris* using seawater as the HTT medium for the first time. Firstly, the influences of the feedstock (microalgae, almond hulls and their binary mixtures) on the yields of products (gas, biocrude, hydrochar, aqueous products) and their critical physicochemical properties (elemental and chemical analyses and heating values) were thoroughly addressed at different processing temperatures (200–300 °C) and times (20–180 min). Secondly, optimum processing parameters were optimized for the individual and joint conversion of both feedstocks into biofuels of different natures, including the individual and/or simultaneous production of liquid and solid biofuels with high calorific values (Fig. 1). The limited number of works attempting the replacement of freshwater with seawater for the co-HTT of lignocellulosic and/or algal biomasses, in combination with the inherent original co-valorization approach followed, demonstrate that this research represents a landmark contribution toward developing less feedstock-dependent and more sustainable and flexible biorefinery processes for biofuels production.

2. Experimental

2.1. Materials

Solvents (chloroform and ethyl acetate) were obtained from Scharlau chemical company. The seawater (supplied by Rioka del Cantábrico, S. L.) was taken from the Matxitxako cape at the Urdaibai biosphere reserve in the Cantabrian Sea (Spain) and filtrated to remove the solids and microorganisms before use. The inorganic chemical composition, pH, and conductivity of the seawater are supplemented in Table S1. The seawater used in the co-HTT experiments contains Na^{+}, Mg^{2+}, Cl^{-}, and SO_4^{2-} in relatively high concentrations (>1000 mg/L). The organic matter in seawater mainly comprises volatile and dissolved organic compounds (Spyres et al., 2000). Total Organic Carbon (TOC) determined the amount of these compounds and a TOC value lower than 1 mg/L was obtained, which agrees with other values reported in the literature (Kameyama et al., 2010; Ogawa and Ogura, 1992). The microalgae *Chlorella Vulgaris* was acquired to Biotiva (Germany) as a fine dehydrated powder and used without additional treatment. Almond hulls were from Marcona-type almonds harvested in Spain. The characteristics, including elemental, biochemical, and proximate composition, of the algae and almond hulls, together with the methodologies followed for their characterization, can be found in the supplementary data (Table S2).

2.2. Co-hydrothermal treatment process

A stainless-steel batch autoclave (300 mL) equipped with a speed-controlled mechanical stirrer (Parker Autoclave Engineers) was used for the hydrothermal experiments (Zhou et al., 2022b). Typically, 18 g of biomass (i.e., algae, almond hulls, or their mixture) and 120 g of seawater were loaded into the autoclave. After checking its airtightness, the reactor was sealed, purged with N_2, and charged with 2 MPa (at room temperature) of pure N_2. However, the initial and final pressure ranges under reaction conditions depend on the reaction temperature, which are 3.8–4.4 MPa at 200 °C, 6.1–7.4 MPa at 250 °C, and 10.6–11.4 MPa at 300 °C. These pressures are higher than the saturation pressure of water at each temperature, which facilitates the hydrothermal process and helps maintain the reaction media in the liquid phase. Finally, the reactor was heated, and the residence time was recorded as soon as the reaction temperature was achieved.

After the reaction, the temperature was decreased to 30–40 °C using cold water to quench the reaction vessel. Then, a gas sample was collected in a gas bag to determine its chemical composition. Afterward, the autoclave was depressurized and opened. Next, the inner wall of the reaction vessel and stirring paddle were rinsed with $CHCl_3$ twice to recover the products. The solid product (hydrochar) and the liquid (biocrude and aqueous fraction) were separated via filtration. Then, the solid was oven-dried at 105 °C overnight. The biocrude was recovered from the aqueous phase following a two-time liquid-liquid extraction procedure using $CHCl_3$ and EtOAc as the extracting solvents. In the final stage, both solvents were removed via first rotary evaporation, followed by further purification with a N_2 stream to recover the biocrude. The graphical experimental procedure is depicted in Fig. 2.

2.3. Analytical methods and response variables

The responses to evaluate the impacts of feedstock composition, processing temperature, and residence time include the product yields and some of their most crucial fuel and chemical properties (Table 1).

The gaseous phase chemical composition was quantified by micro gas chromatography connected to a thermal conductivity detector (Variant CP 4900 GC-TCD) equipped with a Porapack and molecular sieve columns, using He as the carrier gas, and calibrated with a standard gas mixture. The gas yield included the total amounts of gaseous species detected and quantified. The amounts of gas were calculated based on the Ideal Gas Law. An ideal gas behavior at the temperature and pressure at which the gas sample was collected was assumed for this calculation, determining the gas volume as the difference between the inner reactor volume and that of the solid-liquid slurry. (Remón et al., 2021b, 2022b). The lower heating value (LHV) of the gas product was estimated based on the formula developed by Perry and Green (Perry and Green, 2008). The biocrude was dissolved in $CHCl_3$, and its chemical composition was determined on an Agilent 7890 gas chromatograph mass spectrometer (GC-MS) on a DB-17ms column. Biocrude and hydrochar elemental compositions were determined on a Carlo Erba EA1108 Elemental Analyzer, with their HHVs being estimated according to Channiwala and Parikh (Channiwala and Parikh, 2002). The ash content of the biocrude was determined by calcination with air at 850 °C for 1 h, using a ramp time of 8 °C/min to achieve such a temperature.

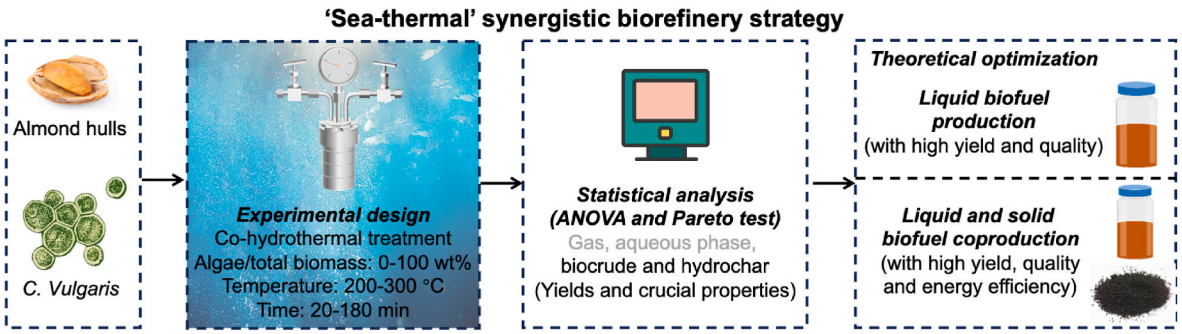

Fig. 1. Novel 'sea-thermal' biorefinery strategy for biofuel production.

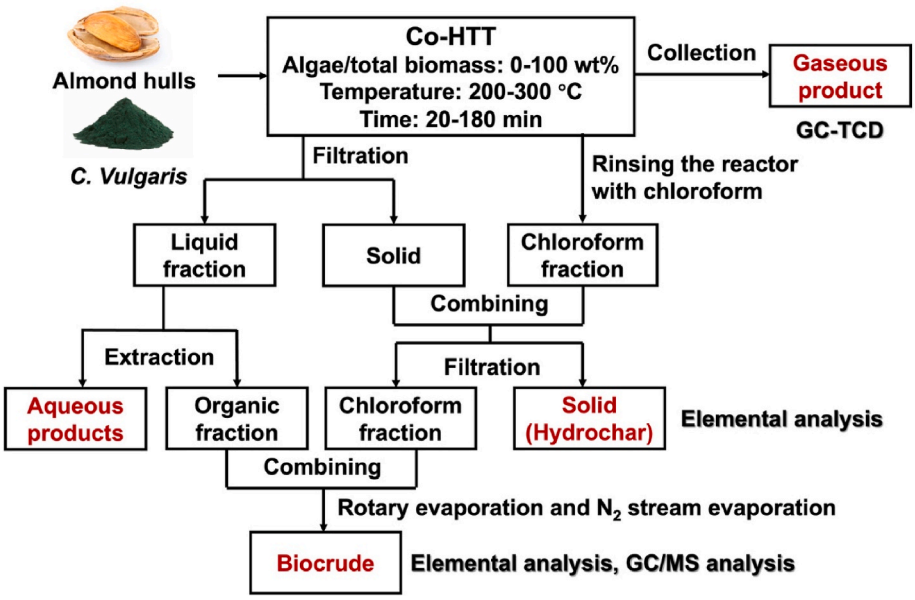

Fig. 2. Schematic diagram of co-HTT experiments.

Table 1
Response variables and methods.

Product	Response variable	Method
Gas	$Gas\ yield\ (\%) = \frac{mass\ of\ gas\ (g)}{mass\ of\ total\ biomass\ (g)} \times 100\%$	GC-TCD
	$Composition\ (\%) = \frac{mol\ of\ each\ gas}{total\ mol\ of\ gas} \times 100\%$	GC-TCD
	LHV (MJ/m^{3}STP) = 0.1079 H_2 (vol%) + 0.1263 CO (vol%) + 0.3581 CH_4 (vol%)	Estimated according to (Perry and Green, 2008)
Biocrude	$Biocrude\ yield\ (\%) = \frac{mass\ of\ biocrude\ (g)}{mass\ of\ total\ biomass\ (g)} \times 100\%$	Gravimetric
	$C,H,O,N\ (\%) = \frac{mass\ of\ C,H,O,N\ (g)}{mass\ ofbiocrude\ (g)} \times 100\%$	Elemental analysis
	HHV (MJ/kg) = 0.3491 C (wt%) + 1.1783 H (wt%) − 0.1034 O (wt%) − 0.015 N (wt%) + 0.1005 S (wt%)	Estimated according to (Channiwala and Parikh, 2002)
	$Composition\ (area\%) = \frac{area\ of\ each\ compound\ (g)}{total\ area\ (g)} \times 100\%$	GC-MS
Hydrochar	$Hydrochar\ yield\ (\%) = \frac{mass\ of\ hydrochar\ (g)}{mass\ of\ total\ biomass\ (g)} \times 100\%$	Gravimetric
	$C,H,O,N\ (\%) = \frac{mass\ of\ C,H,O,N\ (g)}{mass\ ofhydrochar\ (g)} \times 100\%$	Elemental analysis
	HHV (MJ/kg) = 0.3491 C (wt%) + 1.1783 H (wt%) − 0.1034 O (wt%) − 0.015 N (wt%) + 0.1005 S (wt%)	Estimated according to (Channiwala and Parikh, 2002)
Aqueous product	$Aqueous\ yield\ (\%) = 100\% - (gas\ yield + biocrude\ yield + hydrochar\ yield)$	Balance
Energy efficiency	$E(\%) = \frac{gas\ yield \times LHV + biocrude\ yield \times HHV + hydrochar\ yield \times HHV}{algae\ ratio \times algae\ HHV + almond\ hulls\ ratio \times almond\ hulls\ HHV}$	Calculated

2.4. Design of experiments and statistical analysis of the data

A two-level, three-factor (2^3) Box-Wilson (CCF, α: ±1) design was used to plan the co-hydrothermal experiments required to analyze the effects of the feedstock composition (alga/(alga + lignocellulosic), 0–100 wt%), reaction temperature (200–300 °C) and processing time (20–180 min). A biomass/seawater ratio of 15 wt% (g/g) was applied in the co-HTT experiments to achieve a high feedstock handling capacity (high solid/water ratio) under hydrothermal decomposition conditions (Guo et al., 2015; Peterson et al., 2008). This experimental design includes eight runs to determine linear effects and first-order interactions, four repetitions at intermediate conditions (run 9–12) to analyze the experimental error and system variance, and six axial runs to detect quadratic effects and nonlinear interactions (synergistic and antagonistic influences).

An ANOVA (*p-value* < 0.05) was employed to determine the factors significantly influencing the response variables. Besides, the relative importance of these processing parameters was compared through a cause-effect Pareto test. For both analyses, codec variables (from −1 to +1) were utilized to make all the factors comparable. Interaction plots were developed from the formulae based on the ANOVA analysis of the 18 runs performed (Table S4) to graphically address the impact of the processing variables and interactions on the process. These graphs added experimental points to show that the lack of fit is insignificant. In such figures, the least significant difference (LSD) bars are also included to show the experimental errors and system variance. These were determined by the ANOVA of the results, including unexplained variations and statistically significant confidence intervals.

3. Results and discussion

Table S3 summarizes the processing parameters (temperature and

time), and the algae/total biomass ratio (feedstock composition) applied in HTT, together with the obtained experimental data. These results include the global yields of products (i.e., gaseous phase, biocrude, hydrochar, and aqueous fraction) and fundamental physiochemical properties, including elemental and chemical compositions and calorific values. The complete effects of these factors and their interactions on these experimental results based on ANOVA and cause-effect Pareto tests are supplemented in Table S4.

3.1. Overall product formation

The co-HTT of *C. Vulgaris* and almond hulls produces gas (1–5%), hydrochar (6–56%), biocrude (6–55%), and aqueous products (33–52%). CO_2 (>87 vol%) is the main component of the gaseous phase, with low concentrations of H_2 and CO (Table S3), regardless of the feedstock mixture or processing conditions. The cause-effect Pareto tests demonstrate that the yields of hydrochar, biocrude, and aqueous fraction are primarily influenced by the feedstock, i.e., the algae/total biomass ratio (>24%). In comparison, the temperature is the processing parameter that exerts the most significant impact on the gas yield (65%). As for synergies between microalgae and almond hulls, the feedstock (F^2) quadratic terms are statistically significant for the gas, hydrochar, biocrude, and aqueous fraction yields. This significant influence indicates synergies between almond hulls and algae, directing product yields. To address the importance of these synergies (synergetic and antagonistic effects), the ratio of all quadratic effects (F^2) to the total feedstock effects (total linear and quadratic, $F + F^2$) in the models was assessed through the formula $F^2/(F + F^2)$. These data show synergies with importances higher than 15% for the overall yields.

The statistical analysis of the results reveals that the impact of these synergies depends on the HTT temperature and time. In addition to individual impacts, the ANOVA indicates the significant impact of binary interactions between the feedstock composition and the HTT conditions. Oppositely, the potential feedstock-temperature-time interactions do not have an essential contribution. Therefore, their influences are depicted in Fig. 3 using binary interaction plots for the gas, hydrochar, biocrude, and aqueous fraction yields. Particularly, Fig. 3 a/d/g/j plots the influence of the feedstock composition at 200 and 300 °C for a medium reaction time (100 min). Fig. 3 b/e/h/k plots the impact of the reaction temperature as a function of the feedstock composition (algae/total biomass ratio) for 100 min. Fig. 3 c/f/i/l illustrates the impact of the residence time at different temperatures (200–300 °C) for an equimassic feedstock mixture.

3.1.1. Impact of the feedstock mixture

The feedstock composition is a crucial factor directing the overall distribution of products (Fig. 3 a/d/g/j). Despite this variable not significantly impacting the gas yield, it significantly impacts hydrochar,

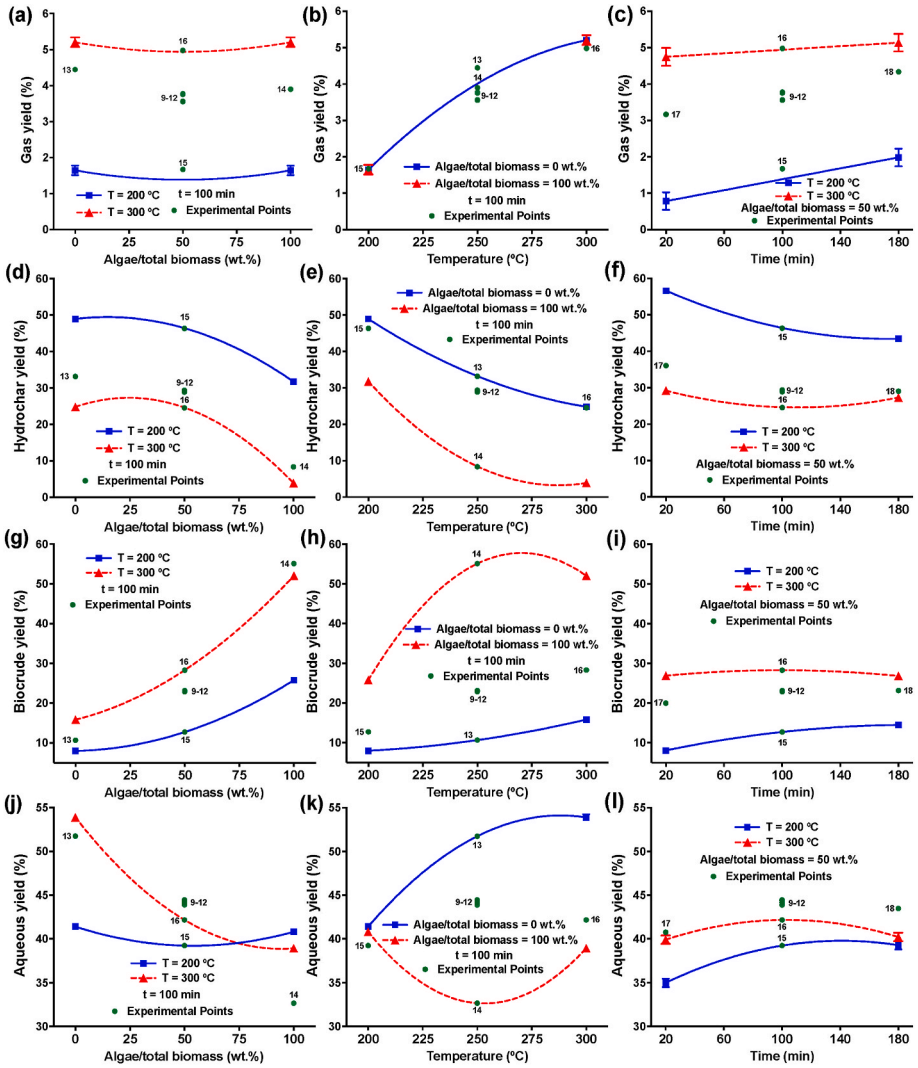

Fig. 3. Impacts of feedstock (almond hulls and algae) and hydrothermal conditions on the product yields. Error bars show LSD intervals.

biocrude, and aqueous fraction yields. As for the gas phase, CO_2 accounts for most gaseous products (88–100 vol%). This suggests that decarboxylation (DCO_2) is the dominant pathway to furnish gaseous products from *C. Vulgaris* and almond hulls. Besides, the impacts on the hydrochar and biocrude yields do not depend on the temperature, while different evolutions take place for the aqueous phase yield. When algae are treated alone, lower hydrochar and higher biocrude are yielded compared to those obtained by processing almond hulls individually, regardless of the temperature. Rising the relative amount of algae (i.e., increasing the algae/total biomass ratio) produces a substantial decrement in the hydrochar yield and a pronounced increment in the biocrude yield. These developments suggest that *almond hulls* are more thermally stable than *C. Vulgaris* under hydrothermal conditions, especially at high processing temperatures, due to the higher volatile content in microalgae than almond hulls. It has also been reported that the lack of lignin in microalgae makes the extraction and conversion of algal components easier compared to lignocellulosic biomass. Besides, saccharides and lignin, with higher proportions in almond hulls, are more prone to undergo carbonization and repolymerization reactions during the HTT process, increasing the hydrochar yield at the expense of biocrude formation (Sahoo et al., 2021; Zhou et al., 2022a).

As described earlier, these variations are not linear, denoting synergistic and antagonistic outcomes between almond hulls and *C. Vulgaris*. Notably, concave decreases in the hydrochar yield occur in parallel with convex increases in the biocrude yield when the ratio of algae to total biomass increases. This indicates synergies between almond hulls and microalgae, which leads to higher hydrochar yields and lower biocrude yields with binary mixture than those theoretically predicted, considering the individual impact of each feedstock in the mixture. As a result, the differences occurring in the production of biocrude and hydrochar with the presence of up to 40 wt% of *C. Vulgaris* in a feedstock containing almond hulls alone are lower than those occurring with rising the amount of *C. Vulgaris* from this step to a feedstock based on algae alone. Such a development indicates that co-processing up to 40 wt% *C. Vulgaris* with almond hulls is a viable option to produce biofuels without altering these yields substantially.

The impact of the feedstock mix on the aqueous fraction yield depends on the temperature. While the feedstock mixture does not affect the liquid yield at 200 °C, increasing the temperature alters the impact of the type of feedstock on the aqueous fraction yield. As a result, at a high temperature (300 °C), a higher aqueous fraction yield is attained with almond hulls than with *C. Vulgaris,* with this yield decreasing convexly by increasing the ratio of this alga to total feedstock. Such developments lead to lower aqueous yields compared to those theoretically predicted, considering each contribution. The temperature impact on the quantity of water-soluble species causes these variations. At a low temperature (200 °C), the HTT of algae or almond hulls in seawater produces similar amounts of water-soluble compounds. Conversely, the HTT of algae at higher temperatures (>200 °C) is more likely to form water-insoluble products than almond hulls. This is because *C. Vulgaris* contains more lipids and proteins but fewer carbohydrates, which favors biocrude formation at the cost of aqueous fraction production (Remón et al., 2021a). Additionally, the decrease observed with increasing the proportion of algae is non-linear, denoting synergistic interactions between almond hulls and *C. Vulgaris* under hydrothermal conditions.

3.1.2. Influence of the processing temperature

The impact of the temperature depends on the type of feedstock composition for the hydrochar, biocrude, and aqueous fraction yields (Fig. 3 b/e/h/k). On the contrary, the impact of this variable on the gas yield does not depend on the feedstock. For this latter fraction, augmenting the reaction temperature significantly increases gas production from 200 to 300 °C regardless of the feedstock. Increasing the temperature decreases the hydrochar yield at the cost of the biocrude and, predominantly, the aqueous fraction yield by processing almond hulls individually. These developments indicate that the reaction temperature facilitates the conversion of almond hulls, whose components are progressively liquefied with increasing temperature, with a substantial amount of aqueous products formed. As stated above, raising the proportion of algae gradually diminishes the hydrochar and aqueous fraction yields by suppressing biocrude production.

For pure algae, augmenting the temperature from 200 to 300 °C links up with an early upsurge and a successive diminution in the biocrude yield, with the highest point at 260–270 °C. These variations occur in parallel with an initial decrease in the aqueous fraction yield in the range of 200–250 °C and a succeeding increase with increasing the temperature to 300 °C. These data suggest that the microalgae are more reactive than almond hulls, which can be easily transformed into biocrude and aqueous products at a moderate temperature. As a result, the hydrochar yield decreases progressively at 200–275 °C, reaching a plateau between 275 and 300 °C. This latter suggests that part of the biocrude is converted to other fractions, including hydrochar, aqueous, and gas species, accounted for by the positive kinetic temperature impact on the repolymerization and DCO_2/decarbonylation (DCO) reactions (Belkheiri et al., 2018; He et al., 2020; Toor et al., 2011).

3.1.3. Impact of the processing time

The impact of HTT time on the reaction products only depends on the processing temperature, with the influence of the feedstock being statistically insignificant. This implies that the effect of the processing time is the same independent of the mix (almond hulls, *C. Vulgaris,* and all possible binary mixtures). As an example, its effect is shown in Fig. 3 c/f/i/l at different temperatures (200–300 °C) for a feedstock comprising equal amounts of almond hulls and *C. Vulgaris*. On the one hand, at 200 °C, raising the processing time increases the gas yield linearly. In parallel, the biocrude and aqueous fraction yields also increase at the hands of the yield to hydrochar. However, these evolutions are particularly important at early reaction stages, i.e., between 20 and 100 min, with meager evolutions occurring further prolonging the duration of the treatment from 100 to 180 min. These evolutions indicate that the processing time exhibits a positive kinetic effect on the dissolution and depolymerization of biomass components, as well as the transformation of the liquid/solid products via DCO_2, DCO, and dehydration reactions (Carpio et al., 2021; Xu and Savage, 2015), regardless of the feedstock used. On the other hand, lengthening the processing time from 20 to 180 min at an elevated temperature (300 °C) modifies the overall product distribution slightly. In detail, the gas yield augments linearly with the increase in processing time. Simultaneously, the biocrude and aqueous yields increase marginally by extending the processing time between 20 and 100 min and subsequently decreasing slightly from 100 to 180 min. Such latter variations occur at the expense of an early rise continued by a succeeding diminishment in the hydrochar yield. The abovementioned results highlight the promotional temperature effect, masking the impact of the processing time for shorter treatments. Besides, using long residence times at a high temperature boosts gasification and repolymerization, yielding more gaseous products and hydrochar.

3.2. Elemental composition and HHV of the biocrude

The proportions of C, H, O, and N in the biocrude vary by 58–67 wt%, 6–8 wt%, 20–35 wt%, and 1–6 wt%, respectively, which turns its HHV from 24 to 31 MJ/kg. A negligible amount of solid matter, lower than the detection limit of the balance, i.e., <0.001 mg, was obtained during the calcination of the biocrude at 850 °C, which indicates that it contains an insignificant amount of ash. This is accounted for by the insolubility of the inorganic seawater salts in the organic solvents (chloroform and ethyl acetate) used to extract the biocrude from the aqueous fraction. The cause-effect Pareto analyses (Table S4) reveal that the feedstock composition, HTT temperature and their interactions influence the elemental contents and HHV of the biocrude significantly, whereas the reaction time little impacts these properties.

As for feedstock synergies, the quadratic terms in the models for the feedstock (F^2) are significant for the percentage of C, H, and O in the biocrude and its HHV, which confirms synergies between the lignocellulosic and the algal biomasses ruling the biocrude elemental composition and HHV. Notably, the $F/(F + F^2)$ ratio denotes synergies between 40 and 50 % for the biocrude elemental contents and HHV. The statistical analysis also shows that the impact of these synergies differs with the HTT temperature and time only, while the possible triple (feedstock-time-temperature) interactions do not contribute to the elemental composition of biocrude. Therefore, Fig. 4 includes binary interaction figures illustrating the influences of the HTT conditions on the biocrude elemental proportions and HHV. Particularly, Fig. 4 a/d/g/j shows the effect of the feedstock mix at different temperatures (200–300 °C) for a middle residence time (100 min). The impact of the hydrothermal temperature as a function of the feedstock mix (algae/total biomass ratio) for 100 min is illustrated in Fig. 4 b/e/h/k. The effect of the reaction time at different temperatures (200–300 °C) for an equimassic feedstock mixture is illustrated in Fig. 4 c/f/i/l.

3.2.1. *Impact of the feedstock mix*

The feedstock significantly affects the elemental contents and HHV of the biocrude, with diverse importances depending on the temperature of the treatment (Fig. 4 a/d/g/j/m). At 200 °C, the biocrude from pure microalgae comprises more significant proportions of C and H and lower contents of O than that resulted from the hydrothermal treatment of almond hulls, with these variations translating in a higher HHV for the former than the latter feedstock. As for binary mixtures, increasing the microalgae proportion from pure almond hulls to a feedstock comprising 75 wt% algae augments the C and H contents accompanied by a drop in the O concentration. A subsequent upsurge from this point to pure algae diminishes the C and H contents of the biocrude slightly. As a result of these evolutions, the HHV of biocrude increases with an initial rise in the

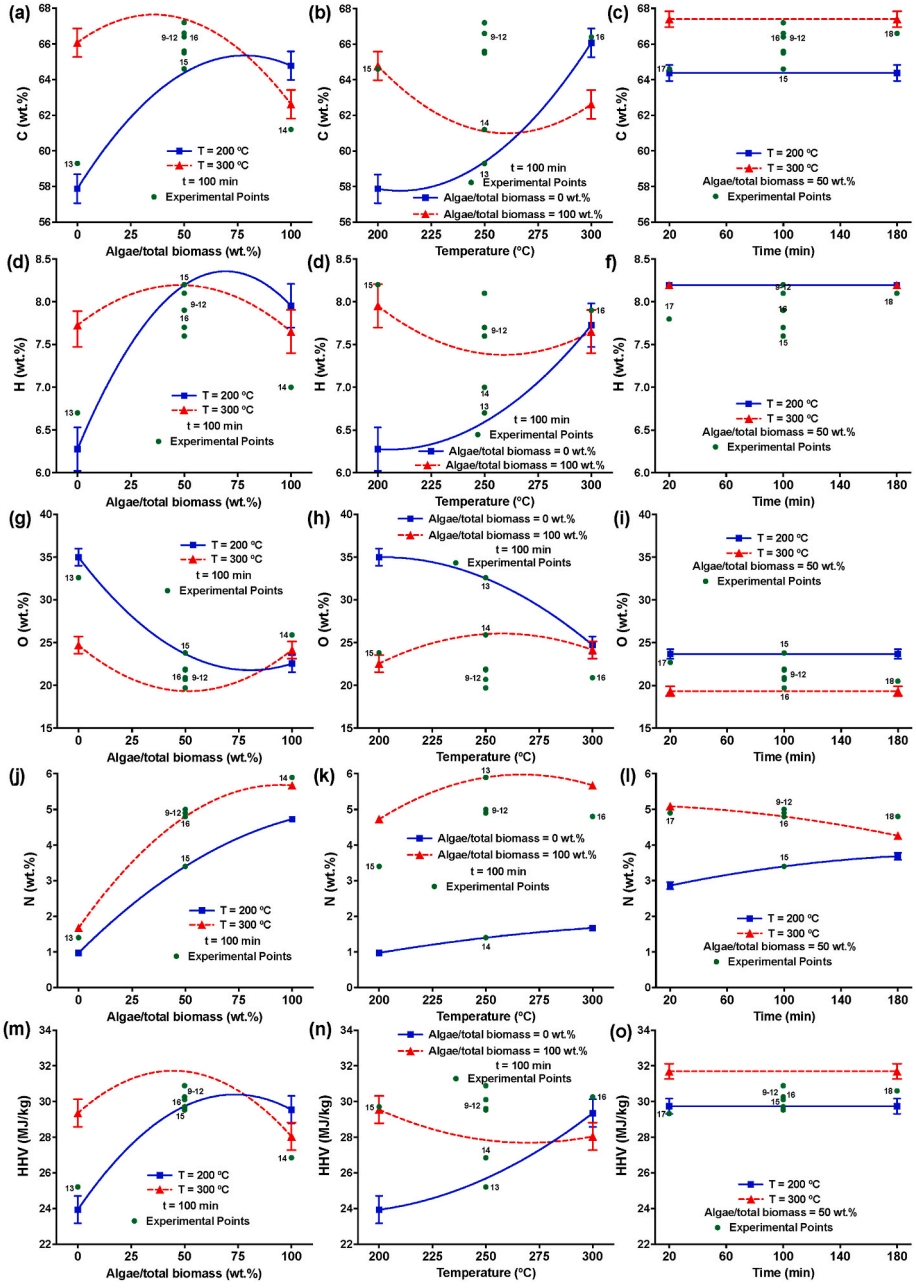

Fig. 4. Impacts of feedstock composition (almond hulls and algae) and HTT conditions on the biocrude elemental composition and HHV. Error bars show least significant difference (LSD) intervals.

microalgae content but decreases subsequently by further switching the feedstock to pure microalgae.

Notably, convex C, H, N, and HHV increments and a concave decrease in the biocrude O concentration occur. Consequently, the actual changes are more pronounced than those theoretically predictable, considering the discrete input of each feedstock in the mixture. This indicates that the microalgae exhibit a synergistic effect on improving the fuel properties of the biocrude produced from almond hulls. These evolutions demonstrate that the synergies between algae and almond hulls promote the deoxygenation reactions (e.g., DCO_2, DCO, and dehydration), eliminating O from biocrude in CO, CO_2, and H_2O. At 300 °C, the impact of the feedstock is less significant. Notably, the biocrude obtained with almond hulls holds a slightly higher amount of C and similar amounts of H and O than that produced from pure algae, which results in a biocrude with a similar HHV regardless of the feedstock. As an exception, increasing the amount of algae in the feedstock increases the N content in the biocrude because of the much higher amount of N in the algae than in the almond hulls. The lesser influence of the feedstock mixture, resulting in less significant synergistic interactions between feedstocks at a higher than at a lower temperature, might be ascribed to the favorable temperature impact on DCO, DCO_2, and dehydration reactions reducing O contents. These reactions are prone to occur at higher temperatures and can mask the impact of the feedstock composition at high temperatures.

3.2.2. Influence of the temperature

The impact of the processing temperature differs depending on the feedstock mix (Fig. 4 b/e/h/k/n), with a more marked effect for almond hulls than for *C.Vulgaris*. For pure almond hulls, increasing the temperature between 200 and 300 °C raises the contents of C, H, and N, accompanied by a drop in the content of O in the biocrude, with these evolutions causing an increment in the biocrude HHV. Two complementary phenomena account for these variations. On the one hand, the significant influence of the temperature on the dissolution and conversion of different almond hull structural components, i.e., O-rich carbohydrates and lignin with relatively high C and H, increases the proportions of these species in the biocrude. On the other, the possible deoxygenation of some dissolved biocrude molecules is promoted by augmenting the temperature, thus decreasing the relative proportion of O (de Caprariis et al., 2017; Tian et al., 2015).

For pure algae, the influence of the reaction temperature is slighter than for almond hulls. This might result from the higher reactivity of this feedstock under hydrothermal conditions, which makes it possible for lower temperatures to achieve a similar conversion degree as that occurring with almond hulls. Notably, augmenting the reaction temperature from 200 to 250 °C declines the contents of C and H but upturns the proportions of O and N, leading to a decrease in the HHV of biocrude. A subsequent increment in the temperature to 300 °C raises the C and H contents at the expense of the O and N proportions, increasing the HHV slightly within this temperature range. These variations indicate that the conversions of microalgal components (i.e., lipids, carbohydrates, and proteins) are progressively promoted by augmenting the temperature, which aligns with the published literature (Zhou et al., 2020). In particular, C and H-rich lipids are dissolved initially at 200 °C, followed by the subsequent dissolution of O-rich saccharides and N-rich proteins between 200 and 250 °C. In addition, increasing the temperature from 250 to 300 °C removes O and N atoms in the microalgal biocrude by deoxygenation and deamination reactions, resulting in an initial decrease and a subsequent increase in the biocrude HHV.

3.2.3. Impact of the processing time

The hydrothermal time does not significantly affect the elemental contents and HHV of the biocrude produced from almond hulls, *C. Vulgaris,* or their mixtures, as stated above. For example, Fig. 4 c/f/i/l/o shows the processing time impact on the elemental composition and HHV of the biocrude using an equimassic mixture at 200 and 300 °C. Despite the temperature, the processing time does not influence the concentrations of C, H, O, or HHV. Exceptionally, the N concentration in the biocrude from almond hulls increases and decreases slightly by extending the processing time at 200 °C and 300 °C, respectively. However, such variations are insignificant from a practical point of view.

3.3. Chemical composition of the biocrude

The biocrude produced from the HTT of *C. Vulgaris*, almond hulls, and their mixtures includes five categories of organic compounds in different proportions (relative chromatographic area): hydrocarbons (0–26%), fatty acids/esters (0–25%), phenols (0–41%), nitrogen-containing compounds (2–89%) and other oxygenated compounds (including alcohols, aldehydes and ketones, 1–54%). Hydrocarbons and fatty acids/esters are mainly derived from lipids in algae and/or almond hulls, phenols are produced from algal protein and/or almond hulls lignin, nitrogen-containing species arise from the hydrolysis of proteins and interactions of proteins with other components, while other oxygenated compounds are mainly derived from the depolymerization and further conversion of saccharides (Chen et al., 2019; Gai et al., 2015; Li et al., 2015).

The complete biocrude chemical composition is supplemented in Table S5. According to the Pareto analysis (Table S4), the feedstock mainly affects the proportions of phenols, other oxygenated compounds, and N-containing compounds. In contrast, the relative amounts of aliphatic compounds (fatty acids/esters and hydrocarbons) primarily depend on the hydrothermal processing temperature. Additionally to these influences, synergies between almond hulls and *C. Vulgaris* take place, as can be numerically calculated considering the quadratic contribution in comparison to the total influence of the feedstock. The ratios $F^2/(F + F^2)$ in the models reveal synergies of 18% for hydrocarbons, 46% for fatty acids/esters, 26% for phenols, 38% for N-containing compounds, and 26% for other oxygenated compounds. Besides, the triple interactions (feedstock-temperature-time) significantly influence the biocrude chemical composition. Thus, the influence of the feedstock mixture is provided as a function of the temperature (200–300 °C) for three different reaction times (20, 100, and 180 min) in Fig. 5 a/d/g/j, b/e/h/k, and c/f/i/l, respectively. Contrarily, this interaction is insignificant for the N-containing species concentration, and the treatment time does not influence the reaction temperature or feedstock composition. As an example, the influence of these two variables on the relative proportion of N-containing compound is plotted for a medium processing time (100 min) in Fig. 5 m.

3.3.1. Influence of the feedstock mixture

The biocrude chemical composition is significantly influenced by the feedstock mixture. This is particularly notorious for the contents of fatty acids/esters, phenols, oxygenated compounds, and N-containing species. On the contrary, the relative amount of hydrocarbons is less directed by the feedstock mixture and more controlled by the temperature and processing time. As for the former, regardless of the reaction temperature (200 or 300 °C) or reaction time (20, 100, and 180 min), higher proportions of phenols and oxygenated compounds are observed in the biocrude obtained from almond hulls than that produced from *C. Vulgaris*. Augmenting almond hulls in the feedstock mix from pure almond hulls to a combination with half of each material results in increases in the relative proportion of fatty acids/esters and N-containing species occurring with drops in the amounts of phenolic and other oxygenated compounds. Contrarily, a further increase in algae amounts drops the relative contents of fatty acids/esters and increases the relative proportion of phenols. These variations follow a non-linear pattern and denote synergistic interactions between biomasses ruling the biocrude chemical composition. The former increases are more pronounced than those theoretically expected, which suggests that the synergistic effect between the algae and almond hulls promotes the dissolution of lipids

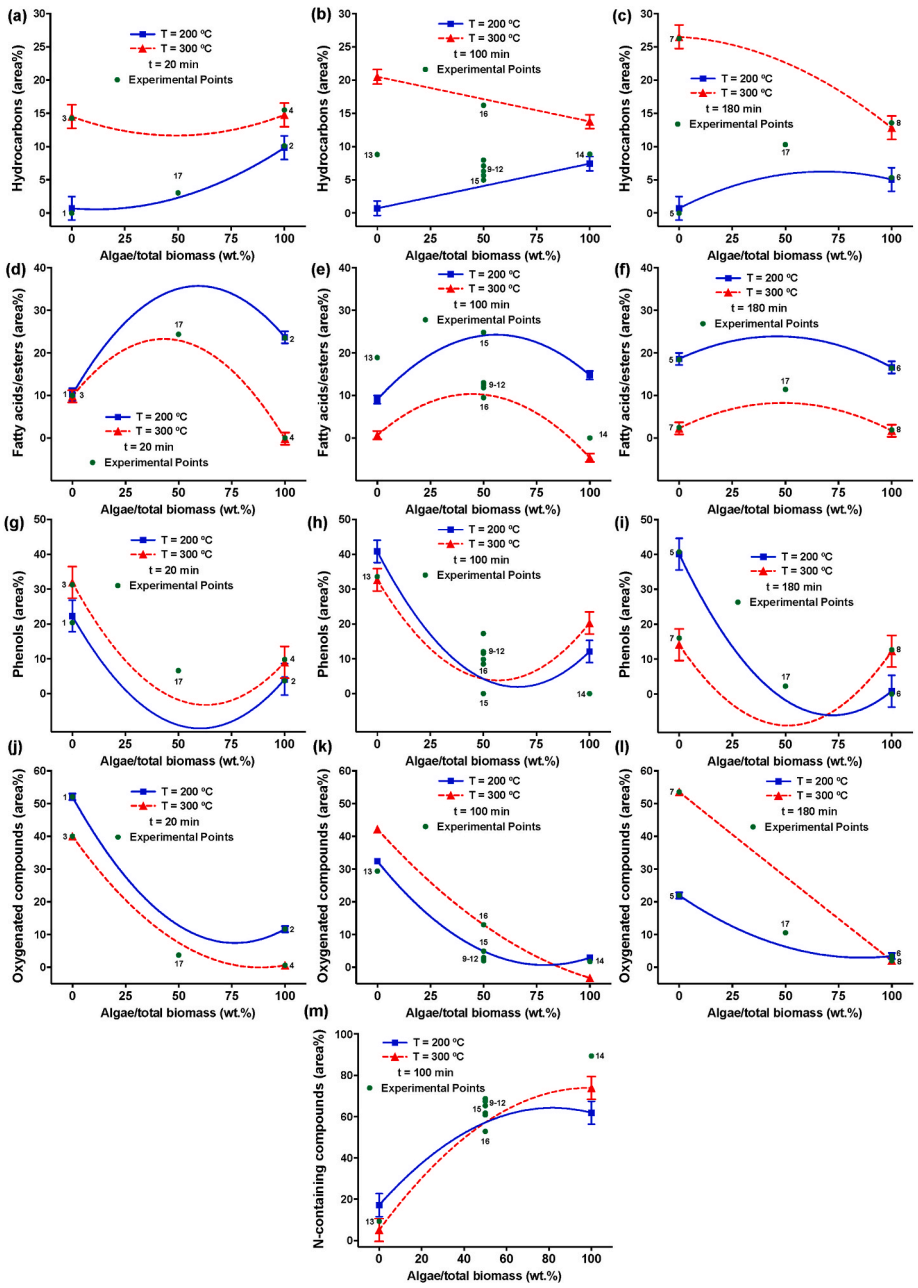

Fig. 5. Impacts of the feedstock composition (algae and almond hulls) on the biocrude chemical composition at 200 and 300 °C for a duration of 20, 100, and 180 min. Error bars show least significant difference (LSD) intervals.

and N-containing species, with this latter effect also accounting for the much higher N content of the algae than the almond hulls. The presence of phenols in the biocrude results from two pathways: (1) the depolymerization of lignin from almond hulls and (2) the deamination of proteins in algae and almond hulls (Chen et al., 2019; Gai et al., 2015; Li et al., 2015). These evolutions suggest that a small amount of algae in the biomass mixture can inhibit the depolymerization of lignin in the almond hull, while the deamination of proteins is promoted by an algae-rich biomass mixture as the feedstock.

With regard to the content of hydrocarbons in the biocrude, the feedstock composition shows different influences depending on the temperature. At 200 °C, an increase in the algae/(algae + almond hulls) ratio raises the relative content of hydrocarbons in the biocrude. At 300 °C, prolonged reaction time changes the variation trend of hydrocarbons by increasing the algae proportion from nearly constant to gradually decreasing. These hydrocarbons are derived from lipids in biomass feedstocks, which are more abundant in microalgae (Sajjadi et al., 2018). At low temperatures, lipid dissolution is the primary hydrocarbon source in biocrude. However, as the temperature increases, other components in microalgae, such as sugars and proteins, are dissolved and converted, which account for a higher proportion of the biocrude. Therefore, the relative content of hydrocarbons in the feedstock decreases slightly as the proportion of microalgae increases.

3.3.2. *Impact of the temperature and reaction time*

As the temperature increases from 200 °C to 300 °C, the relative content of hydrocarbons augments, and the relative proportion of fatty acids/esters decreases, regardless of the biomass composition. This might be due to the fact that rising temperature leads to the transformation of fatty acids/esters into other products, such as nitrogen-containing amides, and the deoxygenation into hydrocarbons (Chen et al., 2019; Liu et al., 2021). When the feedstock mixture contains an

algae proportion up to 50 wt%, the relative proportion of N-containing compounds decreases slightly by augmenting the temperature at 200–300 °C, while the relative proportion of these species augment slightly as the algae proportion increases from 50 to 100 wt%. These variations could be ascribed to the deamination of N-containing species from the co-HTT of a feedstock rich in almond hulls promoted by rising temperature. However, the interaction between N-containing species and other intermediates can be promoted using an algae-abundant biomass mixture as the feedstock, which can generate N-heterocycles and amides (Maillard reaction and acylation reaction) (Cui et al., 2020; He et al., 2020; Zhang et al., 2016).

The influence of reaction temperature on the relative proportions of oxygen-containing compounds and phenols differs depending on the treatment time. For a co-HTT process of 20 min, a rise in the temperature diminishes the relative amounts of O-containing species, irrespective of the lignocellulosic/algal mix. With a 100 min duration, the relative content of O-containing species augments by increasing the temperature. Concerning phenolic compounds, higher temperatures facilitate the formation of phenols for a quick processing time (20 min), irrespective of the feedstock composition. Extending the treatment time to 100 min and 180 min, the conversion of a feedstock with abundant almond hulls results in a slightly decreased phenol relative content by increasing the temperature; increasing the temperature augments the relative proportion of phenols from the co-HTT of an algae-rich feedstock. These phenomena indicate that the dissolution and conversion of most of the structural components in the biomass, except lipids and lignin, is favored by increasing the temperature for a speedy treatment, resulting in a biocrude with a higher relative amount of phenols and a decreased relative content of oxygen-containing compounds. For a long processing time, when an almond-rich feedstock is used, the repolymerization of phenolic compounds is promoted by augmenting the temperature. In addition, increasing the proportion of algae facilitates

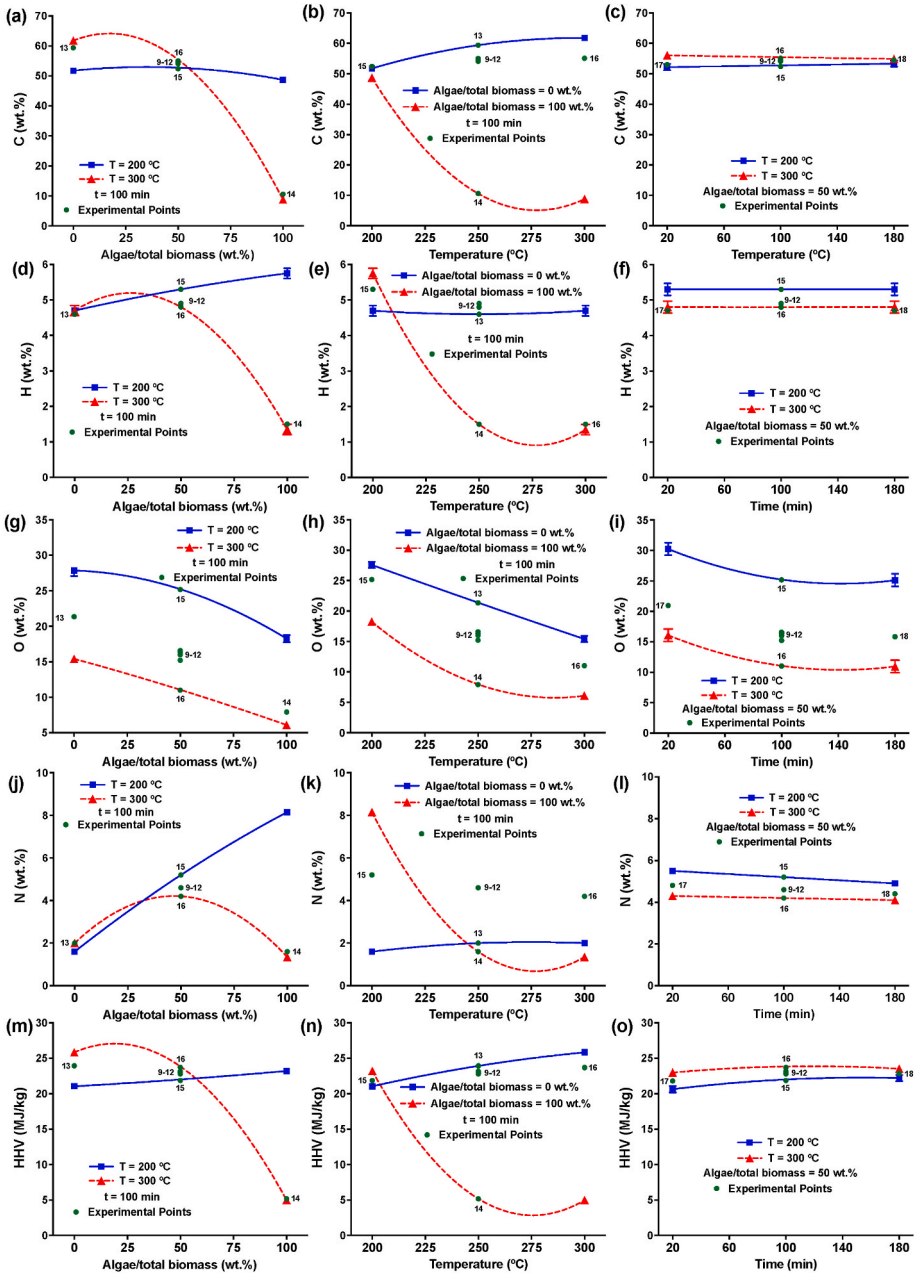

Fig. 6. Impacts of feedstock composition (algae and almond hulls) and processing conditions on the hydrochar properties. Error bars show least significant difference (LSD) intervals.

the deamination of proteins to produce more phenols.

3.4. Elemental composition and HHV of the hydrochar

The relative contents of elements in the hydrochar vary between 5 and 63 wt% C, 1–6 wt% H, 8–31 wt% O, and 1–6 wt% N, with these evolutions altering the HHV from 3 to 26 MJ/kg. Based on the Pareto analysis (Table S4), the feedstock composition, followed by the processing temperature, exhibits the most influential impact on the properties of hydrochar, while the impact of the hydrothermal time is less critical. Besides, the quadratic terms feedstock (F^2) terms are significant for the proportions of C, H, and O in the hydrochar and its HHV, which confirms synergies between materials. Notably, the $F^2/(F + F^2)$ ratio in the models reveals synergies between 30% for all these variables, with the impact of these synergies depending on the temperature and time only. Thus, the feasible feedstock-temperature-time interactions do not have an essential contribution to the elemental distribution, and HHV of hydrochar and binary interaction plots have been created to show the influences of the processing conditions on those properties. Particularly, Fig. 6 a/d/g/j shows the impact of the feedstock composition at different temperatures (200–300 °C) for a medium processing time (100 min). Fig. 6 b/e/h/k plots the impact of the reaction temperature linked with the feedstock composition (algae/total biomass ratio) for a reaction time of 100 min. Fig. 6 c/f/i/l illustrates the effect of the time at different temperatures (200–300 °C) for an equimassic feedstock mixture.

3.4.1. Influence of the feedstock mixture

The influence of the feedstock composition on the elemental composition and HHV of the hydrochar depends on the HTT temperature. At 200 °C, such an impact is not very marked for the contents of C, H, and HHV. Simultaneously, its influence is substantially more critical for N and O. As a result, the hydrochar obtained with pure almond hulls, pure algae, or their mixtures contains similar C and H concentrations. Conversely, the almond hull-derived hydrochar contains a higher amount of O and a lower amount of N than that produced from pure algae. Thus, increasing the amount of *C. Vulgaris* from almond hulls only to a feedstock consisting of pure algae leads to a decrement in the amount of O and an increment in the N content of the hydrochar. These variations follow a linear pattern, indicating that substantial feedstock interactions do not occur at a low temperature. Besides, these evolutions are mainly caused by the slow dissolution/conversion rate at a low reaction temperature and the inherent chemical differences between the feedstocks, i.e., similar C and H contents but higher N and lower O proportions in the microalgae compared to the lignocellulosic material.

At 300 °C, the feedstock composition exerts a more significant impact on the elemental composition and HHV of the hydrochar. The hydrochar obtained from pure almond hulls comprises higher C, H, and O than its equivalent yielded from *C. Vulgaris*. These variations lead to a more energetic hydrochar produced from almond hulls than from the algae. At 300 °C, most of the organic species in microalgae are dissolved and transformed into other products, i.e., biocrude, aqueous, and gaseous products, leaving the solid residue with a large proportion of ash. Therefore, switching the feedstock from almond hulls to algae significantly reduces the elemental organic content and HHV. Accounting for these differences, increasing the proportion of algae in the mix results in drops in the contents of C, H, and O and the HHV of the hydrochar. These variations follow a convex pattern, with the hydrochar obtained containing higher percentages of C, H, O, and N along with a superior HHV than such theoretically probable, considering the specific input of each material in the mixture. As a result, increasing the amount of algae in the feedstock from pure almond hulls to a mixture containing up to 20 wt% of algae does not substantially modify the contents of C or H of the hydrochar. These evolutions confirm interactions between algae and almond hulls, affecting the elemental composition and HHV of the hydrochar. Some of these can promote the dissolution of O-deficient species or the deoxygenation reactions to remove oxygen atoms. As an exception, the N content increases initially and decreases subsequently, while the O content decreases continuously by augmenting the microalgae proportion. These variations are accounted for by the more reactive organic components in the microalga than in almond hulls.

3.4.2. Influence of the temperature

The reaction temperature influences the hydrochar elemental composition and HHV depending on the feedstock composition. As an example, these influences are shown in Fig. 6 b/e/h/k for 100 min. For pure almond hulls, the temperature does not substantially modify the elemental composition or HHV of the hydrochar. Notably, a rise in the temperature between 200 and 300 °C slightly increases the contents of C, H, and N, accompanied by a drop in the O content, with these evolutions following a linear pattern and resulting in a linear increase in the HHV of the hydrochar. These evolutions result from the positive kinetic effect of hydrothermal temperature on the deoxygenation of hydrochar components, as well as the dissolution of O-abundant cellulose and hemicellulose, leaving the lignin fraction with higher C and H contents in the hydrochar (Jamari and Howse, 2012; Li et al., 2018; Lu et al., 2013). Very differently, when *C. Vulgaris* is used as the feedstock, the impact of the hydrothermal temperature is more marked. Mainly, an initial increment in the temperature between 200 and 275 °C decreases the proportions of C, H, N, and O sharply, which diminishes the hydrochar HHV, while a further increase in the temperature to 300 °C does not substantially modify these parameters. These results indicate that *C. Vulgaris* transformation to biocrude, aqueous and gaseous products occurs substantially between 200 and 275 °C, while temperatures higher than 275 °C lead to further transformation of these products, such as the repolymerization and condensation reactions of the liquid products.

3.4.3. Impact of the treatment time

Compared with the two factors mentioned above, the impact of hydrothermal time on the chemical and fuel properties of hydrochar is less influential. Regardless of the temperature and feedstock composition, enlarging the processing time produces a marginal drop in the amount of O in the hydrochar without substantially altering the contents of C, H, N, or the HHV of this solid. These transformations reveal that prolonging processing time favors the deoxygenation reactions (e.g., DCO_2, DCO, and dehydration) of the hydrochar very slightly.

3.5. Theoretical optimization and energy evaluation

Five scenarios were considered to find optimal conditions to furnish biofuels from the co-HTT of *C. Vulgaris* and almond hulls using the empirical formulae derived from ANOVA of the experimental data. Optimizations 1–3 (Opts. 1–3) are aimed at obtaining high-quality liquid biofuel in high yields from *C. Vulgaris*, almond hulls, and their mixtures, maximizing the biocrude yield and its HHV and minimizing the concentration of O and N in the biocrude. Optimization 4 (Opt. 4) is directed to produce a solid biofuel by maximizing the yield and HHV of the hydrochar and minimizing the contents of O and N in this solid, while optimization 5 (Opt. 5) intends to simultaneously produce biocrude and hydrochar with high yield and energy density, considering the previous restrictions. In these optimizations, each constraint was assigned a relative importance (between 1 and 5) to sort out a solution that meets all the different optimization criteria. These optimization conditions, their relative importance, and the optimal results obtained are listed in Table 2. The regression (R^2, $R^2_{adjusted,}$ and $R^2_{predicted}$) coefficients are superior to 0.95, and the models have signal/noise ratios superior to 4 with an insignificant lack of fit (p-value >0.05). Such properties make them appropriate for prediction objectives. Additionally, the experimental and theoretical data for all the runs conducted have been compared, and there are no significant differences with 95% confidence. Also, the theoretical results attained in Opt. 1 and 3 have been corroborated experimentally (Table S6) without finding significant differences

Table 2
Theoretical optimization: restrictions and optimal conditions.

Optimization	1		2		3		4		5	
	Obj.	Solution	Obj.	Solution	Obj.	Solution	Obj.	Solution	Obj.	Solution
Algae/total biomass (wt%)		100	Eq. to 0	0	−(1)	61		22		40
Temperature (°C)		268		300		300		300		300
Time (min)		180		112		108		180		180
Global yields										
Gas (%)		4.90 ± 0.24		5.24 ± 0.24		4.98 ± 0.24		5.22 ± 0.24		5.15 ± 0.24
Hydrochar (%)		4.51 ± 0.26		24.78 ± 0.26		21.77 ± 0.26	+(3)	30.03 ± 0.26	+(3)	29.01 ± 0.26
Biocrude (%)	+(3)	59.23 ± 0.13	+(3)	15.88 ± 0.13	+(3)	32.55 ± 0.13		18.53 ± 0.13	+(3)	23.43 ± 0.13
Aqueous (%)		31.69 ± 0.27		53.91 ± 0.27		40.71 ± 0.27		45.89 ± 0.27		41.93 ± 0.27
Biocrude elemental composition and HHV										
N (wt%)	−(4)	5.90 ± 0.06	−(4)	1.68 ± 0.06	−(4)	5.14 ± 0.06		3.00 ± 0.06	−(4)	3.88 ± 0.06
C (wt%)		61.06 ± 0.79		66.08 ± 0.79		66.87 ± 0.79		67.41 ± 0.79		67.62 ± 0.79
H (wt%)		7.39 ± 0.24		7.73 ± 0.24		8.16 ± 0.24		8.06 ± 0.24		8.18 ± 0.24
O (wt%)	−(4)	25.93 ± 1.00	−(4)	24.71 ± 1.00	−(4)	19.51 ± 1.00		21.09 ± 1.00	−(4)	19.59 ± 1.00
HHV (MJ/kg)	+(5)	27.69 ± 0.76	+(5)	29.35 ± 0.76	+(5)	31.41 ± 0.76		31.12 ± 0.76	+(5)	31.71 ± 0.76
Hydrochar elemental composition and HHV										
N (wt%)		0.21 ± 0.00		2.00 ± 0.00		3.99 ± 0.00	−(4)	3.58 ± 0.00	−(4)	4.10 ± 0.00
C (wt%)		2.34 ± 0.66		61.92 ± 0.66		48.52 ± 0.66		64.58 ± 0.66		59.84 ± 0.66
H (wt%)		0.81 ± 0.12		4.73 ± 0.12		4.34 ± 0.12		5.31 ± 0.12		5.11 ± 0.12
O (wt%)		8.16 ± 0.53		15.24 ± 0.53		9.80 ± 0.53	−(4)	13.61 ± 0.53	−(4)	11.79 ± 0.53
HHV (MJ/kg)		1.04 ± 0.19		25.91 ± 0.19		21.13 ± 0.19	+(5)	27.13 ± 0.19	+(5)	25.48 ± 0.19
Biocrude chemical composition (area%)										
Hydrocarbons		7.44 ± 1.24		21.41 ± 1.24		16.90 ± 1.24		25.55 ± 1.24		23.89 ± 1.24
Fatty acids/esters		2.05 ± 0.74		0.19 ± 0.74		8.40 ± 0.74		6.43 ± 0.74		8.05 ± 0.74
Phenols		0 ± 3.47		31.13 ± 3.47		3.59 ± 3.47		0 ± 3.47		0 ± 3.47
Other oxygenated compounds		4.13 ± 0.42		43.28 ± 0.42		9.30 ± 0.42		42.14 ± 0.42		32.80 ± 0.42
N-containing compounds		87.12 ± 6.22		5.12 ± 6.22		63.88 ± 6.22		32.34 ± 6.22		49.61 ± 6.22
Energy efficiency										
E (%)		75.91		67.05		75.29		78.62		79.56

Objectives: + and – represent maximizing and minimizing, respectively. Numbers in brackets are relative optimization importances.

between both data with 95% confidence. All these analyses validate the statistical models developed in this work for prediction purposes.

Opt. 1 shows that the best biocrude in terms of quantity and quality, i.e., a biocrude yield of 59 % and HHV of 28 MJ/kg, is obtained with pure *C. Vulgaris,* when the hydrothermal treatment is performed at 268 °C for 180 min, leading to an energy efficiency of 76 %. This aligns well with the higher reactivity of the algae than that of the almond hulls for biocrude production, as reported in the previous sections. Given the superior behavior of *C. Vulgaris* for liquid biofuel production, Opt. 2 and 3 explore the possibility of including almond hulls into the feedstock mixture without substantially decreasing liquid biofuel production. First, Opt. 2 reveals that pure almond hulls can furnish a similar biofuel in terms of HHV (29 MJ/kg) but with a much lower biocrude yield (16 %) when optimum processing conditions are applied (300 °C and 112 min), leading to an energy efficiency of only 67%. In parallel, Opt. 3 reveals that this low biocrude yield can be increased up to 33 %, with a high calorific value and energy efficiency (31 MJ/kg and 75%, respectively), including up to 61 wt% of *C.Vulgaris* into the feedstock mixture (61 wt% *C. Vulgaris* + 39 wt% almond hulls). These optimizations suggest that the interaction between *C. Vulgaris* and almond hulls can improve the yield and quality of biocrude to a certain extent, which allows for improving biocrude production from almond hulls. For solid biofuel, a high-energy dense hydrochar (27 MJ/kg) can be obtained in high yield (30 %) from a biomass mixture containing 22 wt% of *C. Vulgaris* and 78 wt% of almond hulls at 300 °C for 180 min (Opt. 4). Additionally, Opt. 5 reveals that it is possible to produce energy-dense liquid (23% biocrude yield and HHV = 32 MJ/kg) and solid (29 wt% hydrochar yield and HHV = 25 MJ/kg) biofuels simultaneously with the co-HTT of a mixture comprising of 40 wt% *C. Vulgaris* and 60 wt% almond hulls, at 300 °C for 180 min, leading to energy efficiency of 80%.

3.6. Mechanistic insights in co-HTT of algal and lignocellulosic biomass and sustainability of the process

The H/C, O/C, and N/C atomic ratios of *C. Vulgaris* and almond hull feedstocks are illustrated in Fig. 7a and b. The H/C, O/C, and N/C ratios of biocrude range from 1.43 to 1.46, 0.22–0.32, and 0.02–0.08, while these ratios of hydrochar range from 0.92 to 1.07, 0.15–0.18, 0.03–0.08, respectively. The results indicate that the transformation of feedstocks to biocrudes includes deoxygenation mechanisms (DCO, DCO_2, and dehydration reactions) (Kabir and Khalekuzzaman, 2022; Khalekuzzaman et al., 2024). Besides, the transformation of biocrudes to hydrochars undergoes a typical mechanism of dehydration reaction, suggesting the condensation/repolymerization of biocrude into hydrochar. As for Fig. 7 b, the variations in H/C and N/C ratio indicate that the denitrogenation reactions (mainly deamination) and interactions of N-species with other components (i.e., carbohydrates and lipids) occur during the conversion of microalgae and almond hulls to biocrude and hydrochar (Tang et al., 2016). These results are consistent with the discussion in Sections 3.2, 3.3, and 3.4.

The proposed reaction pathways are shown in Fig. 7 c based on the abovementioned results. During co-HTT, the main components in microalgae (lipids, carbohydrates, and proteins) and almond hulls (carbohydrates and lignin) dissolved and degraded into fatty acids, amino acids, monosaccharides, and phenols, with the aid of seawater. The salts in seawater could promote the formation of carboxylic acids (formic and acetic acids) from the degradation of polysaccharides at a low temperature (200 °C) (Jiang et al., 2018a, 2018b). These acidic species exhibit autocatalytic effects on the degradation of proteins, resulting in a positive synergistic effect on N-containing species formation in the biocrude (Fig. 4 j). The formed amino acids undergo three main pathways: (1) deamination to carboxylic acids and ammonia, which reacts with fatty acids forming fatty amides; (2) decarboxylation to CO_2 and amine, which reacts with fatty acid forming secondary amides; (3) dimerization to N-heterocycles. The synergy between the two feedstocks promotes the deamination reaction to form carboxylic acids, resulting in the convex variation in the fatty acid/ester relative composition (Fig. 5). Besides, the repolymerization/condensation reactions of the formed monomers are promoted by the synergies between microalgae and almond hulls, leading to the enhancement in hydrochar

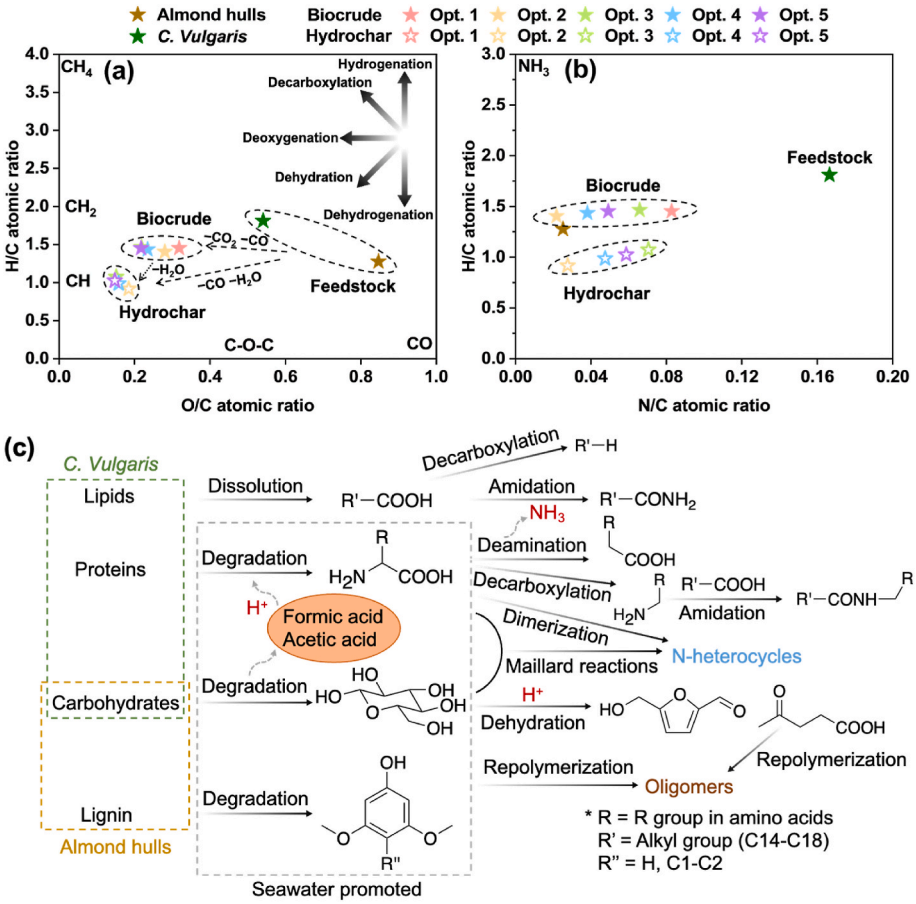

Fig. 7. Van Krevelen diagrams of *C. Vulgaris*, almond hulls, biocrude, and hydrochar obtained under optimized conditions: (a) O/C–H/C; and (b) N/C–H/C. (c) Possible reaction pathways during co-HTT.

formation at a high temperature.

4. Conclusions

This work has addressed the synergetic, 'sea-thermal' (using seawater at hydrothermal conditions) co-processing of almond hulls and *C. Vulgaris* (lignocellulosic and algal biomasses) for biofuel production. The effect of the mixture (synergistic and antagonistic interactions between the biomasses) and the impacts of the processing parameters (reaction temperature and time) were addressed systematically. As for the impact of the feedstock mix, the experimental results demonstrated that growing the amount of microalgae in the mix promotes biocrude production while treating feedstock mixtures with high proportions of almond hulls facilitates the formation of hydrochar and aqueous fraction. The degradation of abundant polysaccharides in almond hulls produced acidic species, promoting the degradation of proteins to N-containing species in biocrude. The synergies between microalgae and almond hulls favored the deamination of amino acid and repolymerization of formed monomers. Additionally, boosting the temperature and lengthening the processing time facilitates the conversion of hydrochar into gas and biocrude. These processing factors also alter the biocrude and hydrochar physicochemical and fuel properties, with improved products obtained from the co-valorization of both feedstocks compared to those obtained with the individual treatment of each biomass.

Process optimization revealed that the HTT of *C. Vulgaris* at 268 °C for 180 min led to the best biocrude production in terms of quantity and quality (59% biocrude yield and HHV = 28 MJ/kg), while almond hulls at optimum conditions (300 °C and 112 min) also furnished an energy-dense biocrude (29 MJ/kg) but in a much lesser yield (16%). However, synergies between materials not only allow increasing this low biocrude yield up to 33%, including up to 61 wt% of *C. Vulgaris* into the feedstock mixture, maintaining the calorific value of the product (31 MJ/kg), but also developing holistic and integrated processes for complete biomass utilization. As for this latter, the co-HTT of 40 wt% *C. Vulgaris* and 60 wt % almond hulls at 300 °C for 180 min resulted in energy-dense liquid (23% biocrude yield and HHV = 32 MJ/kg) and solid (29% hydrochar yield and HHV = 25 MJ/kg) biofuels produced simultaneously, achieving an energy feedstock recovery of 80%. In addition, the aqueous phase from the process could be recycled for another HTT run as the solvent. This takes advantage of the autocatalytic effect of the remaining salts and improves product yield and quality due to the organic species in the aqueous phase (Liu et al., 2022; Picone et al., 2024). This potential aqueous phase recirculation strategy might enhance the sustainability of the process. Besides, different thermochemical processes, such as aqueous phase reforming and/or steam reforming, might be sustainable options to convert the organic content of the aqueous phase into a rich-hydrogen gas, decreasing the organic matter of this effluent to negligible levels to be discharged to the environment and/or used again as a solvent for another hydrothermal treatment. These promising prospects create exciting new avenues to develop novel and synergetic approaches for biomass and waste valorization using seawater as the reaction medium.

CRediT authorship contribution statement

Yingdong Zhou: Writing – original draft, Methodology, Investigation, Formal analysis, Data curation. **Javier Remón:** Writing – review & editing, Supervision, Methodology, Investigation, Funding acquisition,

Formal analysis, Data curation, Conceptualization. **Wei Ding:** Writing – review & editing, Validation, Investigation. **Zhicheng Jiang:** Writing – review & editing, Validation, Methodology, Investigation, Formal analysis. **José Luis Pinilla:** Writing – review & editing, Resources, Investigation, Formal analysis. **Changwei Hu:** Writing – review & editing, Validation, Supervision, Project administration, Funding acquisition, Formal analysis. **Isabel Suelves:** Writing – review & editing, Supervision, Resources, Project administration, Investigation, Funding acquisition.

Declaration of competing interest

The authors declare that they have no known competing financial interests or personal relationships that could have appeared to influence the work reported in this paper.

Data availability

Data will be made available on request.

Acknowledgments

This work was funded by MCIN/AEI/10.13039/501100011033 (I + D + i project PID2020-115053RB-I00) and by the Aragón Government (Research Group Reference T06-23R). This work was also financially supported by the National Natural Science Foundation of China (No. 21536007), the 111 project (B17030), and the Beijing Nova Program (Z211100002121085). Yingdong Zhou acknowledges the support from the China Scholarship Council (CSC No. 202006240156). Javier Remón is grateful to the Spanish Ministry of Science, Innovation and Universities for the Juan de la Cierva (JdC) fellowship (Grant Number IJC2018-037110-I) and thanks MCIN/AEI/10.13039/501100011033 and the European Union « NextGenerationEU»/PRTR » for the Ramón y Cajal Fellowship (RYC2021-033368-I) awarded, and the Aragón Government (Research Group Reference T22_23R) for providing frame support.

Appendix A. Supplementary data

Supplementary data to this article can be found online at https://doi.org/10.1016/j.jclepro.2024.142719.

References

Belkheiri, T., Andersson, S.-I., Mattsson, C., Olausson, L., Theliander, H., Vamling, L., 2018. Hydrothermal liquefaction of kraft lignin in subcritical water: influence of phenol as capping agent. Energy Fuels 32 (5), 5923–5932.
Carpio, R.B., Zhang, Y., Kuo, C.-T., Chen, W.-T., Schideman, L.C., de Leon, R., 2021. Effects of reaction temperature and reaction time on the hydrothermal liquefaction of demineralized wastewater algal biomass. Bioresour. Technol. Rep. 14, 100679.
Channiwala, S., Parikh, P., 2002. A unified correlation for estimating HHV of solid, liquid and gaseous fuels. Fuel 81 (8), 1051–1063.
Chen, X., Peng, X., Ma, X., Wang, J., 2019. Investigation of Mannich reaction during co-liquefaction of microalgae and sweet potato waste. Bioresour. Technol. 284, 286–292.
Cui, Z., Cheng, F., Jarvis, J.M., Brewer, C.E., Jena, U., 2020. Roles of Co-solvents in hydrothermal liquefaction of low-lipid, high-protein algae. Bioresour. Technol. 310, 123454.
Dandamudi, K.P.R., Muppaneni, T., Sudasinghe, N., Schaub, T., Holguin, F.O., Lammers, P.J., Deng, S., 2017. Co-liquefaction of mixed culture microalgal strains under sub-critical water conditions. Bioresour. Technol. 236, 129–137.
de Caprariis, B., De Filippis, P., Petrullo, A., Scarsella, M., 2017. Hydrothermal liquefaction of biomass: influence of temperature and biomass composition on the bio-oil production. Fuel 208, 618–625.
Dimitriadis, A., Bezergianni, S., 2017. Hydrothermal liquefaction of various biomass and waste feedstocks for biocrude production: a state of the art review. Renew. Sustain. Energy Rev. 68, 113–125.
Domínguez de María, P., 2013. On the use of seawater as reaction media for large-scale applications in biorefineries. ChemCatChem 5 (7), 1643–1648.
Elliott, D.C., Biller, P., Ross, A.B., Schmidt, A.J., Jones, S.B., 2015. Hydrothermal liquefaction of biomass: developments from batch to continuous process. Bioresour. Technol. 178, 147–156.
Fakudze, S., Chen, J., 2023. A critical review on co-hydrothermal carbonization of biomass and fossil-based feedstocks for cleaner solid fuel production: synergistic effects and environmental benefits. Chem. Eng. J. 457, 141004.
Fang, C., Thomsen, M.H., Brudecki, G.P., Cybulska, I., Frankaer, C.G., Bastidas-Oyanedel, J.R., Schmidt, J.E., 2015. Seawater as alternative to freshwater in pretreatment of date palm residues for bioethanol production in coastal and/or arid areas. ChemSusChem 8 (22), 3823–3831.
Gai, C., Li, Y., Peng, N., Fan, A., Liu, Z., 2015. Co-liquefaction of microalgae and lignocellulosic biomass in subcritical water. Bioresour. Technol. 185, 240–245.
Galadima, A., Muraza, O., 2018. Hydrothermal liquefaction of algae and bio-oil upgrading into liquid fuels: role of heterogeneous catalysts. Renew. Sustain. Energy Rev. 81, 1037–1048.
Grande, P.M., Bergs, C., Dominguez de Maria, P., 2012. Chemo-enzymatic conversion of glucose into 5-hydroxymethylfurfural in seawater. ChemSusChem 5 (7), 1203–1206.
Guo, Y., Yeh, T., Song, W., Xu, D., Wang, S., 2015. A review of bio-oil production from hydrothermal liquefaction of algae. Renew. Sustain. Energy Rev. 48, 776–790.
He, S., Zhao, M., Wang, J., Cheng, Z., Yan, B., Chen, G., 2020. Hydrothermal liquefaction of low-lipid algae Nannochloropsis sp. and Sargassum sp.: effect of feedstock composition and temperature. Sci. Total Environ. 712, 135677.
Hongthong, S., Raikova, S., Leese, H.S., Chuck, C.J., 2020. Co-processing of common plastics with pistachio hulls via hydrothermal liquefaction. Waste Manage. (Tucson, Ariz.) 102, 351–361.
Hu, Y., Feng, S., Bassi, A., Xu, C., 2018. Improvement in bio-crude yield and quality through co-liquefaction of algal biomass and sawdust in ethanol-water mixed solvent and recycling of the aqueous by-product as a reaction medium. Energy Convers. Manag. 171, 618–625.
Hu, Y., Gong, M., Feng, S., Xu, C., Bassi, A., 2019. A review of recent developments of pre-treatment technologies and hydrothermal liquefaction of microalgae for bio-crude oil production. Renew. Sustain. Energy Rev. 101, 476–492.
Jamari, S.S., Howse, J.R., 2012. The effect of the hydrothermal carbonization process on palm oil empty fruit bunch. Biomass Bioenergy 47, 82–90.
Jiang, Z., Budarin, V.L., Fan, J., Remón, J., Li, T., Hu, C., Clark, J.H., 2018a. Sodium chloride-assisted depolymerization of xylo-oligomers to xylose. ACS Sustain. Chem. Eng. 6 (3), 4098–4104.
Jiang, Z., Fan, J., Budarin, V.L., Macquarrie, D.J., Gao, Y., Li, T., Hu, C., Clark, J.H., 2018b. Mechanistic understanding of salt-assisted autocatalytic hydrolysis of cellulose. Sustain. Energy Fuels 2 (5), 936–940.
Jin, B., Duan, P., Xu, Y., Wang, F., Fan, Y., 2013. Co-liquefaction of micro- and macroalgae in subcritical water. Bioresour. Technol. 149, 103–110.
Kabir, S.B., Khalekuzzaman, M., 2022. Co-liquefaction of organic solid waste with fecal sludge for producing petroleum-like biocrude for an integrated waste to energy approach. J. Clean. Prod. 354, 131718.
Kameyama, S., Tanimoto, H., Inomata, S., Tsunogai, U., Ooki, A., Takeda, S., Obata, H., Tsuda, A., Uematsu, M., 2010. High-resolution measurement of multiple volatile organic compounds dissolved in seawater using equilibrator inlet–proton transfer reaction-mass spectrometry (EI–PTR-MS). Mar. Chem. 122 (1–4), 59–73.
Khalekuzzaman, M., Fayshal, M.A., Adnan, H.M.F., 2024. Production of low phenolic naphtha-rich biocrude through co-hydrothermal liquefaction of fecal sludge and organic solid waste using water-ethanol co-solvent. J. Clean. Prod. 436, 140593.
Leng, L., Zhang, W., Peng, H., Li, H., Jiang, S., Huang, H., 2020. Nitrogen in bio-oil produced from hydrothermal liquefaction of biomass: a review. Chem. Eng. J. 401.
Li, H., Wang, S., Yuan, X., Xi, Y., Huang, Z., Tan, M., Li, C., 2018. The effects of temperature and color value on hydrochars' properties in hydrothermal carbonization. Bioresour. Technol. 249, 574–581.
Li, L.-l., Zhang, R., Tong, D.-m., Hu, C.-w., 2015. Fractional pyrolysis of algae and model compounds. Chin. J. Chem. Phys. 28 (4), 525–532.
Li, Q., Yuan, X., Hu, X., Meers, E., Ong, H.C., Chen, W.-H., Duan, P., Zhang, S., Lee, K.B., Ok, Y.S., 2022. Co-liquefaction of mixed biomass feedstocks for bio-oil production: a critical review. Renew. Sustain. Energy Rev. 154, 111814.
Liu, L., Zhou, Y., Guo, L., Li, G., Hu, C., 2021. Production of nitrogen-containing compounds via the conversion of natural microalgae from water blooms catalyzed by ZrO2. ChemSusChem 14 (18), 3935–3944.
Liu, T., Jiao, H., Yang, L., Zhang, W., Hu, Y., Guo, Y., Yang, L., Leng, S., Chen, J., Chen, J., Peng, H., Leng, L., Zhou, W., 2022. Co-hydrothermal carbonization of cellulose, hemicellulose, and protein with aqueous phase recirculation: insight into the reaction mechanisms on hydrochar formation. Energy 251, 123965.
Lu, X., Pellechia, P.J., Flora, J.R., Berge, N.D., 2013. Influence of reaction time and temperature on product formation and characteristics associated with the hydrothermal carbonization of cellulose. Bioresour. Technol. 138, 180–190.
Nigam, P.S., Singh, A., 2011. Production of liquid biofuels from renewable resources. Prog. Energy Combust. Sci. 37 (1), 52–68.
Obeid, F., Chu Van, T., Brown, R., Rainey, T., 2019. Nitrogen and sulphur in algal biocrude: a review of the HTL process, upgrading, engine performance and emissions. Energy Convers. Manag. 181, 105–119.
Ogawa, H., Ogura, N., 1992. Comparison of two methods for measuring dissolved organic carbon in sea water. Nature 356 (6371), 696–698.
Ong, H.C., Chen, W.-H., Farooq, A., Gan, Y.Y., Lee, K.T., Ashokkumar, V., 2019. Catalytic thermochemical conversion of biomass for biofuel production: a comprehensive review. Renew. Sustain. Energy Rev. 113, 109266.
Ong, H.C., Chen, W.-H., Singh, Y., Gan, Y.Y., Chen, C.-Y., Show, P.L., 2020. A state-of-the-art review on thermochemical conversion of biomass for biofuel production: a TG-FTIR approach. Energy Convers. Manag. 209, 112634.
Perry, R.H., Green, D.W., 2008. Perry's Chemical Engineers' Handbook. McGraw-Hill, New York.

Peterson, A.A., Vogel, F., Lachance, R.P., Fröling, M., Antal, J.M.J., Tester, J.W., 2008. Thermochemical biofuel production in hydrothermal media: a review of sub- and supercritical water technologies. Energy Environ. Sci. 1 (1), 32–65.
Picone, A., Volpe, M., Codignole Luz, F., Malik, W., Volpe, R., Messineo, A., 2024. Co-hydrothermal carbonization with process water recirculation as a valuable strategy to enhance hydrochar recovery with high energy efficiency. Waste Manage. (Tucson, Ariz.) 175, 101–109.
Remón, J., Danby, S.H., Clark, J.H., Matharu, A.S., 2020. A new step forward nonseasonal 5G biorefineries: microwave-assisted, synergistic, Co-depolymerization of wheat straw (2G biomass) and laminaria saccharina (3G biomass). ACS Sustain. Chem. Eng. 8 (33), 12493–12510.
Remón, J., Latorre-Viu, J., Matharu, A.S., Pinilla, J.L., Suelves, I., 2021a. Analysis and optimisation of a novel 'almond-refinery' concept: simultaneous production of biofuels and value-added chemicals by hydrothermal treatment of almond hulls. Sci. Total Environ. 765, 142671.
Remón, J., Ravaglio-Pasquini, F., Pedraza-Segura, L., Arcelus-Arrillaga, P., Suelves, I., Pinilla, J.L., 2021b. Caffeinating the biofuels market: effect of the processing conditions during the production of biofuels and high-value chemicals by hydrothermal treatment of residual coffee pulp. J. Clean. Prod. 302, 127008.
Remón, J., Zapata, G., Oriol, L., Pinilla, J.L., Suelves, I., 2022a. A novel 'sea-thermal', synergistic co-valorisation approach for biofuels production from unavoidable food waste (almond hulls) and plastic residues (disposable face masks). Chem. Eng. J. 449.
Remón, J., Zapata, G., Oriol, L., Pinilla, J.L., Suelves, I., 2022b. A novel 'sea-thermal', synergistic co-valorisation approach for biofuels production from unavoidable food waste (almond hulls) and plastic residues (disposable face masks). Chem. Eng. J. 449, 137810.
Sahoo, A., Saini, K., Jindal, M., Bhaskar, T., Pant, K.K., 2021. Co-Hydrothermal Liquefaction of algal and lignocellulosic biomass: status and perspectives. Bioresour. Technol. 342, 125948.
Sajjadi, B., Chen, W.-Y., Raman, A.A.A., Ibrahim, S., 2018. Microalgae lipid and biomass for biofuel production: a comprehensive review on lipid enhancement strategies and their effects on fatty acid composition. Renew. Sustain. Energy Rev. 97, 200–232.
Seshasayee, M.S., Savage, P.E., 2021. Synergistic interactions during hydrothermal liquefaction of plastics and biomolecules. Chem. Eng. J. 417, 129268.
Shao, Y., Tsang, D.C.W., Shen, D., Zhou, Y., Jin, Z., Zhou, D., Lu, W., Long, Y., 2020. Acidic seawater improved 5-hydroxymethylfurfural yield from sugarcane bagasse under microwave hydrothermal liquefaction. Environ. Res. 184, 109340.
Sharma, K., Castello, D., Haider, M.S., Pedersen, T.H., Rosendahl, L.A., 2021. Continuous co-processing of HTL bio-oil with renewable feed for drop-in biofuels production for sustainable refinery processes. Fuel 306, 121579.
Spyres, G., Nimmo, M., Worsfold, P.J., Achterberg, E.P., Miller, A.E., 2000. Determination of dissolved organic carbon in seawater using high temperature catalytic oxidation techniques. TrAC, Trends Anal. Chem. 19 (8), 498–506.
Tang, X., Zhang, C., Li, Z., Yang, X., 2016. Element and chemical compounds transfer in bio-crude from hydrothermal liquefaction of microalgae. Bioresour. Technol. 202, 8–14.
Tian, C., Liu, Z., Zhang, Y., Li, B., Cao, W., Lu, H., Duan, N., Zhang, L., Zhang, T., 2015. Hydrothermal liquefaction of harvested high-ash low-lipid algal biomass from Dianchi Lake: effects of operational parameters and relations of products. Bioresour. Technol. 184, 336–343.
Toor, S.S., Rosendahl, L., Rudolf, A., 2011. Hydrothermal liquefaction of biomass: a review of subcritical water technologies. Energy 36 (5), 2328–2342.
Xu, D., Savage, P.E., 2015. Effect of reaction time and algae loading on water-soluble and insoluble biocrude fractions from hydrothermal liquefaction of algae. Algal Res. 12, 60–67.
Xu, Y., Ramanathan, V., Victor, D.G., 2018. Global warming will happen faster than we think. Nature 564 (4), 30–32.
Yang, J., He, Q., Yang, L., 2019. A review on hydrothermal co-liquefaction of biomass. Appl. Energy 250, 926–945.
Yang, J., Nasirian, N., Chen, H., Niu, H., He, Q., 2022. Hydrothermal liquefaction of sawdust in seawater and comparison between sodium chloride and sodium carbonate. Fuel 308, 122059.
Zhang, C., Tang, X., Sheng, L., Yang, X., 2016. Enhancing the performance of Co-hydrothermal liquefaction for mixed algae strains by the Maillard reaction. Green Chem. 18 (8), 2542–2553.
Zhou, Y., Chen, Y., Li, M., Hu, C., 2020. Production of high-quality biofuel via ethanol liquefaction of pretreated natural microalgae. Renew. Energy 147, 293–301.
Zhou, Y., Hu, C., 2020. Catalytic thermochemical conversion of algae and upgrading of algal oil for the production of high-grade liquid fuel: a review. Catalysts 10 (2), 145.
Zhou, Y., Liu, L., Li, G., Hu, C., 2021. Insights into the influence of ZrO2 crystal structures on methyl laurate hydrogenation over Co/ZrO2 catalysts. ACS Catal. 11 (12), 7099–7113.
Zhou, Y., Liu, L., Li, M., Hu, C., 2022a. Algal biomass valorisation to high-value chemicals and bioproducts: recent advances, opportunities and challenges. Bioresour. Technol. 344, 126371.
Zhou, Y., Remón, J., Gracia, J., Jiang, Z., Pinilla, J.L., Hu, C., Suelves, I., 2022b. Toward developing more sustainable marine biorefineries: a novel 'sea-thermal' process for biofuels production from microalgae. Energy Convers. Manag. 270, 116201.
Zhou, Y., Remón, J., Gracia, J., Jiang, Z., Pinilla, J.L., Hu, C., Suelves, I., 2022c. Toward developing more sustainable marine biorefineries: a novel 'sea-thermal' process for biofuels production from microalgae. Energy Convers. Manag. 270.
Zhou, Y., Remón, J., Pang, X., Jiang, Z., Liu, H., Ding, W., 2023. Hydrothermal conversion of biomass to fuels, chemicals and materials: a review holistically connecting product properties and marketable applications. Sci. Total Environ. 886, 163920.